Chapter 7
One-Dimensional Nanowire-Based Heterostructures for Gas Sensors

Jun Zhang and Xianghong Liu

7.1 Introduction

Gas sensors with the ability to detect gaseous species in a quantitative and qualitative manner play an important role in various aspects in our daily lives. They can function as a feasible means to monitor air quality, environmental pollution, chemical detection, control of chemical processes, food quality, and medical diagnosis and so forth.

One-dimensional (1D) nanostructures at least one dimension in the range of 1–100 nm (nanowires, nanorods, nanoribbons or nanobelts, nanofibers) have long been considered as promising building blocks for gas sensors [1–7]. The fascinating features of nanowires for gas sensing include high surface-to-volume ratio, sensitive surface, high crystallinity, high carrier mobility, low power consumption and ease for device integration [2, 6, 8, 9]. In 2001 nanowires were initially employed to fabricate gas sensors as proof-of-concept [2, 3]. Afterwards nanowires are drawing fast growing interest in the field of gas sensing with an outcome of over 1200 publications in past 15 years from the Web of Science using the keywords nanowire and gas sensor (Fig. 7.1). It is important to note that among these publications metal oxide nanowires hold a dominant position, while other nanowires including organic polymers, metals, and other semiconductors only register a small part (12.6%). It is not strange that n-type ZnO and SnO_2 nanowires are the most extensively studied materials for gas sensing because the electron mobility in ZnO and SnO_2 is very high (160 and 200 $cm^2\ V^{-1}\ s^{-1}$, respectively) with respect to that of other metal oxides such as In_2O_3, WO_3 and TiO_2 (100, 10 and 0.4 $cm^2\ V^{-1}\ s^{-1}$, respectively)

J. Zhang (✉) · X. Liu
College of Physics, Qingdao University, Qingdao, China
e-mail: jun@qdu.edu.cn; xianghong.liu@qdu.edu.cn

© Springer Nature Singapore Pte Ltd. 2019

G. Shen, Y.-L. Chueh (eds.), *Nanowire Electronics*, Nanostructure Science and Technology, https://doi.org/10.1007/978-981-13-2367-6_7

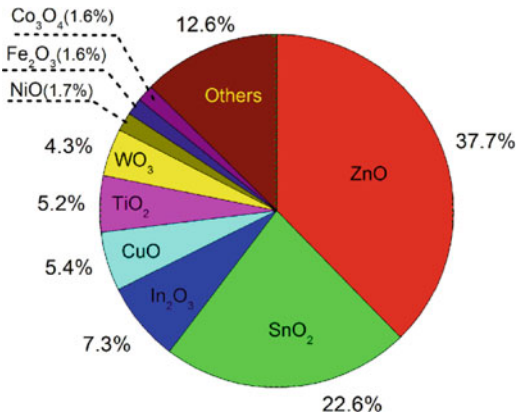

Fig. 7.1 Research on metal oxide nanowires for gas sensors. (From Web of Knowledge, July 2016)

[8]. Although p-type semiconductor metal oxides such as CuO, NiO, Co_3O_4 with low hole mobility only take part of lower than 10% for gas sensing, [10] they can function in high-performance gas sensor by forming heteronanostructures or serving as a catalyst.

1D metal oxide nanostructures were first utilized for gas sensor in 2002, when Comini et al. [11] and Yang et al. [4] demonstrated respectively that single-crystalline SnO_2 nanobelts (nanoribbons) prepared by thermal evaporation were highly sensitive to NO_2. Kolmakov et al. [12] were among the first to show SnO_2 nanowires obtained by using AAO template method exhibited highly sensitive, fast, stable, and reproducible reponses to CO. In 2003, the Zhou group [13] initially reported In_2O_3 nanowires-based field-effect transistor (FET) as a gas sensor to detect NO_2 and NH_3 with significantly improved sensing performance in comparison with the traditional thin-film based sensors. Later in 2004, Wan et al. [14] reported that ZnO nanowire sensors exhibited a very high sensitivity to ethanol and fast response time at 300 °C. Following these early works, research on nanowire sensors has been attracting more and more interest.

In order to improve the sensing properties of nanowires, significant efforts have been directed to sensitize the nanowire surface. By now typical strategies include decorating nanowire surface with secondary-phase nanoparticles, [15–22] forming core-shell structures, [23–26] and elemental doping [27–29]. Among these methods, surface functionalization of 1D nanowire with various nanoparticles (metals, oxides, semiconductors) has attracted considerable interest because of synergistic benefits induced by the coupling and the heterointerface between the host nanowires and guest nanoparticles. Such a nanowire-nanoparticle heterostructure have been shown to greatly improve the "4S" gas sensing parameters, e.g. sensitivity, selectivity, stability, speed (response-recovery time), as well as the operating temperature.

In this chapter, we will specially focus on the progress made in the past 15 years toward using the unique nanowire-nanoparticle heterostructures for achieving superior sensing performance. Since in the field of gas sensing there have been many comprehensive reviews and chapters dealing with synthesis, modification and

application of 1D nanostructure for sensors, [6–9, 30–38] we do not attempt another chapter as such here. The major goal is to identify how one can optimize the above-mentioned gas sensing characteristics through engineering nanowire-nanoparticle heterostructures and contribute to the understanding of function mechanisms for heteronanowire-based gas sensors.

7.2 Advantages of Nanowires for Application in Gas Sensing

As a typical 1D nanostructure, nanowires can offer some essential advantages over nanoparticles for gas sensing [8]. Conventional gas sensing film consists of a large quantity of nanoparticles, which have a risk of grain coarsening induced by the high working temperature. This might cause a decreased stability of the sensor device as the polycrystalline sensitive layer might be sintered due to thermal effects after a long working. This has been proved by Sysoev et al., [39] who carried out a comparative study of the long-term gas sensing performance of single crystal SnO_2 nanowires and SnO_2 nanoparticles (Fig. 7.2a, b). They showed that the device made of nanowires demonstrated excellent sensitivity and long-term stability toward traces of 2-propanol in air. Different from the nanowires, the nanoparticles exhibited a superior initial sensitivity, but the sensitivity deteriorated during the first month of operation and gradually stabilized at the level observed steadily in the nanowires. The enhanced stability of the nanowire sensors is ascribed to the reduced propensity of the nanowires to sinter under real operation conditions with respect to

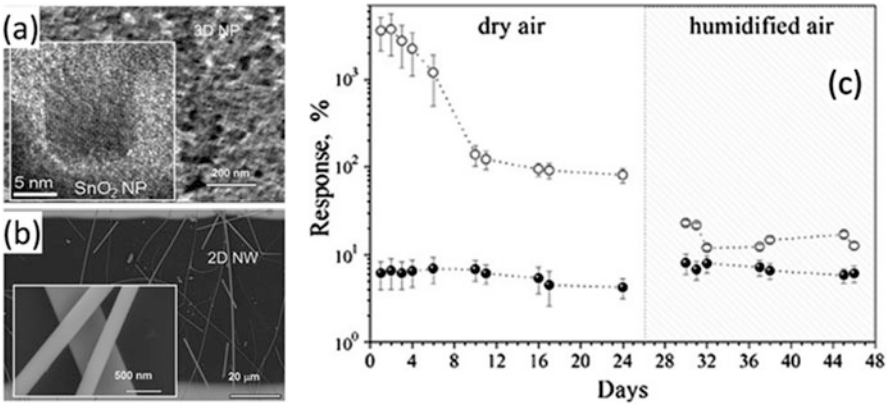

Fig. 7.2 HRTEM and SEM images of (**a**) SnO_2 nanoparticle layer and (**b**) SnO_2 nanowires, (**c**) the change of sensor baseline resistance measured with SnO_2 nanoparticles and SnO_2 nanowires versus time. Open and filled circles correspond to nanoparticles and nanowires. Experiments were initially carried out in dry air and then (since day 26) in humified air. Reproduced from ref. [39], Copyright 2009, with permission of Elsevier

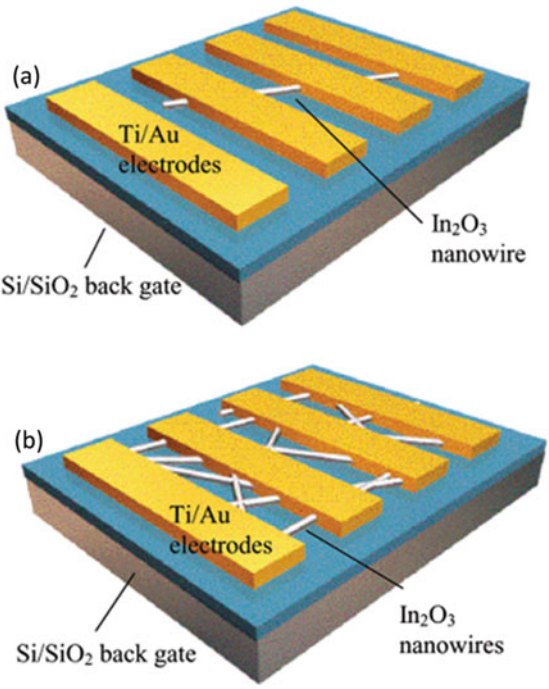

Fig. 7.3 Scheme of gas sensors based on (**a**) a single nanowire transistor and (**b**) multi-nanowires. Reproduced from ref. [40]. Copyright 2004 American Chemical Society

nanoparticles. Long-term working at elevated operating temperature facilitates sintering of nanoparticles, leading to aggregation and encapsulation of nanoparticles into larger agglomerates. This work also reveals that the humidity has very big influence on the sensor stability of nanoparticles, while nanowires possess a relative good resistance to humidity.

Another advantage of nanowires is that they can be directly employed as the sensing element in a single nanowire form (Fig. 7.3a) [40]. In a single nanowire sensor, the nanowire must be carefully positioned on electrodes. Compared to nanowire films (Fig. 7.3b), fabrication of sensor devices based on a single nanowire requires the use of more complex and multiple processes, as well as high fabrication cost.

However, single nanowire sensors afford the opportunity to fully utilize the unique features of 1D nanostructure, e.g., the very thin diameter, large surface-to-volume ratio, and high crystalline quality. Kolmakov et al. [12] demonstrated that for SnO_2 nanowires with a diameter of 60 nm the surface adsorption of molecules could alter the bulk electronic properties of the nanowire, not merely the surface region.

Furthermore, in a single nanowire device, the effects coming from nanowire–nanowire interfaces are avoided, which plays an important role in conventional sensors based on polycrystalline nanoparticle and nanowire films. The absence of such crystallite interfaces ensure the successful realization of a conductivity switch, the bulk conductivity of which is fully determined by the surface sensing behavior.

This offers the base for researchers to study the intrinsic sensing mechanism arising from the surface chemistry occurring on a nanowire.

7.3 Nanowire–Nanoparticle Heterostructures and Gas Sensing Mechanism

Nanowires can function as a sensing element in many sensor configurations [38] such as chemiresistors, Field-effect transistors (FET), optical sensors, surface acoustic wave sensors and quartz crystal microbalance sensors, among which the chemiresistor whose conductance is altered by charge-transfer processes occurring at their surfaces and FET whose properties is controlled by applying an appropriate potential onto its gate are commonly used for investigation of sensing features of nanowires [6, 7].

The fundamental operating principles of gas sensing have been explained in many publications. Briefly electrical conductivity or resistivity of materials is modified by the sensing reactions between ionosorbed oxygen species and gas molecules. The gas sensing reactions induce charge transfer, which alters the conductance or resistance of the materials. The sensing reactions taking place on material surface usually involve mainly three processes, i.e. adsorption, reaction, and desorption. Take n-type metal oxides such as ZnO, SnO_2, and In_2O_3 for example (Fig. 7.4a),

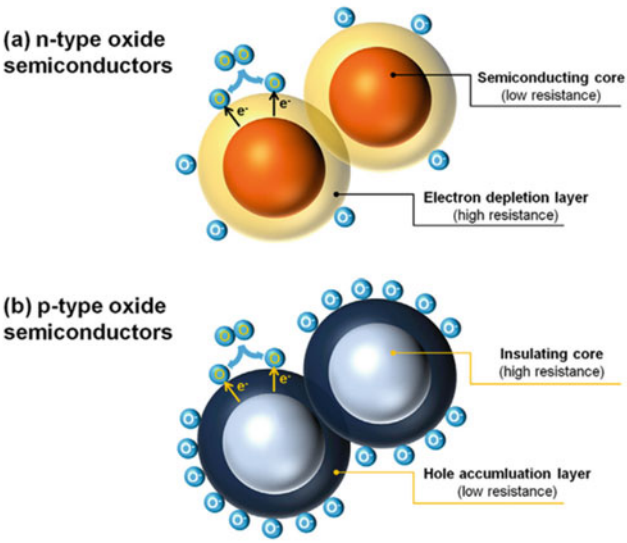

Fig. 7.4 Formation of (**a**) electron depletion layer in n-type and (**b**) hole accumulation layer in p-type oxide semiconductors. Reproduced from ref. [10], Copyright 2014,with permission of Elsevier

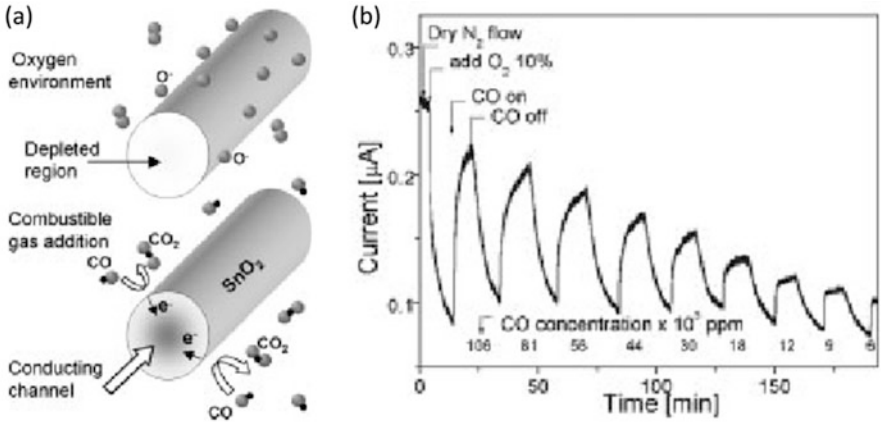

Fig. 7.5 The sensing mechanism of SnO_2 nanowires involves (**a**) a completely depleted and hence nonconductive state under an oxidizing ambient and sharply increased conductance due to electron transfer from surface states back into the nanowires interior when a reducing gas (CO) is admitted. (**b**) The response of the nanowires toward O and CO pulses. The CO concentration in the flowing gas was reduced from pulse to pulse. Reproduced from ref. [12] with permission of Wiley-VCH

oxygen molecules adsorb onto the surface of semiconductors and ionize into chemisorbed oxygen species such as O_2^-, O^-, and O^{2-} by drawing electrons from the surfaces of the semiconductors [41, 42]. In general, it is believed that the chemisorbed oxygen species of O_2^-, O^-, and O^{2-} are dominant at <150 °C, between 150 and 400 °C, and at >400 °C, respectively [42]. This process creates an electron depletion layer and turns the semiconductor into a high resistive state [42]. While for p-type metal oxide semiconductors (Fig. 7.4b), this leads to the formation of hole accumulation layer near the surface. Exposure to reductive gases such as ethanol will result in an increase in the conductivity for n-type semiconductors and a decrease for p-type materials, whereas the effect of oxidative gases is reversed.

1D metal oxide nanowires with a typically high length-to-diameter ratio are regarded as promising candidates for high-performance sensor. Based on the well-known grain size effect [43], sensor sensitivity is critically related to the grain size (D) of nanoparticles when D is comparable to 2 L (L is the thickness of electron depletion layer or space charge layer). When D is larger than 2 L, only the grain boundary is subject to formation of electron depletion layer, meaning that the sensing reactions do not change the sensor resistance very much. From this perspective the diameter of nanowires should have an important effect on gas sensing performances. For example, Kolkamov et al. [12] stated that not only the surface region but also the entire SnO_{2-} nanowire could be depleted of electrons if the diameter is small enough, i.e. comparable to the Debye length (ca. 43 nm for SnO_2 at 500 K). In air rich of oxygen, the SnO_2 nanowires are non-conductive because the nanowire is fully depleted of conduction electrons (Fig. 7.5a). Exposure to

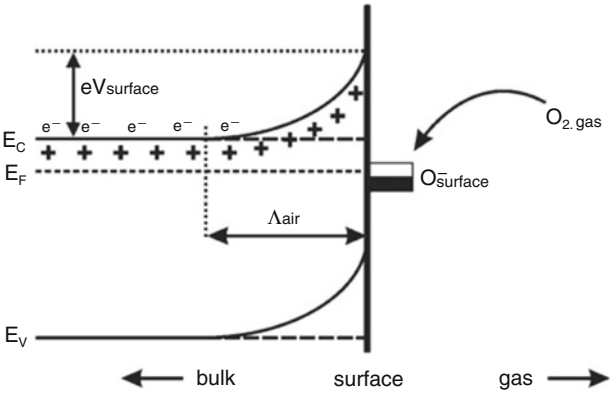

Fig. 7.6 Illustration of band bending in a wide bandgap semiconductor after chemisorption of charged oxygen species on surface sites. E_C, EV, and E_F denote the energy of the conduction band, valence band, and the Fermi level, respectively, while Λ_{air} denotes the thickness of the space-charge layer, and $eV_{surface}$ the potential barrier. The conducting electrons are represented by e^- and + represents the donor sites. Reproduced from ref. [22] with permission of Wiley-VCH

combustible gas such as CO switches the SnO_2 nanowires into conductive state again. Their sensing properties shown in Fig. 7.5b are also consistent with this mechanism.

The adsorption of the charged oxygen species leads to band bending (Fig. 7.6), which generates a surface potential barrier eV_s. The height (eV_s) and depth (w) of the band bending depend on the surface charge concentrations, [22, 44] which is determined by the amount and type of adsorbed oxygen. The conductance of nanowires can be defined as [31, 38, 42].

$$G = n_0 e \mu \pi \frac{(D - 2w)^2}{4L}$$

where n_0 is the concentration of charge carriers, e the electron charge, μ the mobility of the electrons, D and L are the diameter and length of the nanowire channel, w the depth of electron depletion layer which is related to the Debye length of materials. The Debye length is obtained in Schottky approximation [42].

$$w = \lambda \sqrt{\frac{eV_s}{kT}}$$

$$\lambda = \sqrt{\frac{\varepsilon \varepsilon_0 kT}{e^2 n_0}}$$

where V_S is the band bending induced by chemisorption of charged species, ε_0 the absolute dielectric constant, ε the relative dielectric permittivity of the structure, k the

Bolzmann's constant, T the temperature. The change in conductance induced by the surface sensing process can be expressed as

$$\Delta G = \Delta n_s e \mu \pi \frac{(D - 2w)^2}{4L}$$

Therefore the sensor sensitivity (S, in some cases *sensitivity* is also named as *Response* [11]) can be defined as

$$S = \frac{\Delta G}{G} = \frac{\Delta n_s}{n_0}$$

where Δn_s is the change in concentration of charge carriers. The linear dependence of S on Δn_s reveals that a more measurable change in concentration of charge carriers can enhance the sensor sensitivity. Great effort is thus focused on manipulating the Δn_s through surface functionalization of metal oxide nanowires.

Although metal oxide semiconductor holds a dominant position in gas sensing, they suffer from some critical drawbacks such as poor selectivity and high operating temperature. The past 15 years has witnessed significant advance in sensor performance propelled by sensor scientists. Numerous efforts have approved the effectiveness of surface functionalization of nanowires by nanoparticles as a sensitizer or promotor toward optimizing the "4S" sensor parameters, i.e., sensitivity, selectivity, stability, and speed, as well as operating temperature. In the following section we will mainly discuss the unique heteronanowires being composed of nanowires as the host and guest nanoparticles, and their sensing mechanism. Based on the functionalization materials, the guest phase are classified as metal nanoparticles and metal oxide nanoparticles.

7.3.1 Metal Oxide–Metal Heteronanowires

To date, great success has been achieved in employing noble metal nanoparticles as a promotor to sensitize the surface of metal oxide semiconductors for enhanced gas sensing. Metal nanoparticles can be loaded onto metal oxides to give the heterostructures by various physical or chemical techniques [45, 46]. Table 7.1 summarizes some typical gas sensors based on 1D Metal oxide-Metal nanostructures.

From Table 7.1, it is seen noble metals such as Au, Ag, Pd, and Pt have been widely used as a promotor. However the promotion mechanisms are quite different based on the used metals. According to Yamazoe, [43] the "promotion effect" by noble metals can be classified as "chemical sensitization" or "electronic sensitization", depending on whether the noble metals change the work function of the semiconductor or not. The chemical sensitization (Fig. 7.7a) takes place via a

Table 7.1 Properties of gas sensors based on 1D metal oxide-metal nanostructures

Materials	Test gas	Concentration (ppm)	Sensitivity (S)/ Response (R)	Detection limit (ppm)	Temperature (°C)
Pd/ZnO nanowires [21]	H_2S	10	732.1	< 1	265
Pd/ZnO nanowires [47]	Ethanol	500	61.5%	< 5	230
ZnO/Au nanowires [48]	CO	50	60%	< 5	250
ZnO/Pt nanowires [49]	NO_2	0.1	1.08	< 0.1	100
Pd/ZnO nanowire [50]	Acetone	500	153.8	–	300
ZnO/Au nanowires [51]	Ethanol	100	33.6	< 2	380
Au/ZnO nanorods [52]	H_2S	3	475	< 1	25
Au/ZnO nanowires [53]	Benzene	10	6.275	< 1	340
Au/ZnO nanowires [54]	H_2S	1	38	1	25
Au/ZnO nanorods [55]	Ethanol	100	52.5	< 1	310
Au/ZnO nanowires [56]	Ethanol	5	1.33	< 5	325
Ag/ZnO nanowires [57]	Ethanol	10	6	1	280
Au/ZnO nanorods [58]	NO_2	2	16 (S)	500 ppb	150
Pt/ZnO nanowires [59]	Ethanol	50	32.6	250 ppb	265
Pd/ZnO nanorods [60]	CO	1000	4.6	–	300

(continued)

Table 7.1 (continued)

Materials	Test gas	Concentration (ppm)	Sensitivity (S)/ Response (R)	Detection limit (ppm)	Temperature (°C)
Au/ZnO nanorods [61]	CO	200	3.4 (S)	–	150
Pt/SnO_2 nanowires [62]	H_2	100	13	–	150
Pt/SnO_2 nanorods [63]	Ethanol	200	39.5	< 10	300
Pt/SnO_2 nanowires [64]	Toluene	1	40	< 1	300
Pt/SnO_2 nanowires [65]	CO	400	7	1	400
Pd/SnO_2 nanorods [66]	Ethanol	500	5.9	–	300
Pd/SnO_2 nanofibers [67]	Formaldehyde	100	18.8	–	160
Rh/SnO_2 nanofibers [68]	Acetone	50	60.6	< 1	200
Ag/SnO_2 nanowires [69]	NO_2	1	>1000	–	300
Pd/SnO_2 nanorods [70]	H_2	10	2.85	–	350
Au/SnO_2 nanowires [71]	NO_2	60	10	0.1	300
Pd/SnO_2 nanofibers [72]	H_2	1	2.57	20 ppb	160
Pt/In_2O_3 nanofibers [73]	H_2S	600	1490	–	200
Pt/In_2O_3 nanowires [74]	O_2	15	1.04	–	50
Au/In_2O_3 nanowires [75]	CO	5	104	< 0.2	Room temp.

(continued)

Table 7.1 (continued)

Materials	Test gas	Concentration (ppm)	Sensitivity (S)/ Response (R)	Detection limit (ppm)	Temperature (°C)
Au/In_2O_3 nanorods [76]	Acetone	50	40	10 ppb	250
Pd/In_2O_3 nanowires [16]	NO_2	30	8	< 3	300
Au/In_2O_3 nanowires [77]	CO	100	2200	500 ppb	Room temp.
Ag/TiO_2 nanobelts [78]	Ethanol	20	6.659	–	200
Pd/TiO_2 nanobelts	Ethanol	10	7.16	–	200
Pt/TiO_2 nanowires [79]	CO	30	1.18	–	300
Pd/TiO_2 nanowires [80]	H_2	1000	7	–	100
Pd/TiO_2 nanowires [81]	Chloroform	1000	0.65	–	200
Pd/TiO_2 nanorods [82]	H_2	1000	250	–	30
Au/WO_3 nanorods [83]	H_2	50	6.6	–	290
Pt/WO_3 nanorods [84]	Ethanol	200	7.3	< 1	220
Pd/WO_3 nanorods [85]	NH_3	100	5	–	300
Pd/WO_3 nanotubes [86]	H_2	500	17.6	< 10	450
Au/WO_3 nanowires [87]	H_2S	10	80	< 5	291
Ru/WO_3 nanorods [88]	H_2S	10	192	0.2	350

(continued)

Table 7.1 (continued)

Materials	Test gas	Concentration (ppm)	Sensitivity (S)/ Response (R)	Detection limit (ppm)	Temperature (°C)
Pd/WO_3 nanowires [89]	H_2	1000	3	–	300
Au/Fe_2O_3 nanowires [90]	Acetone	1	5.91	< 1	270
Au/Fe_2O_3 nanorods [91]	Butanol	100	9.5	–	320

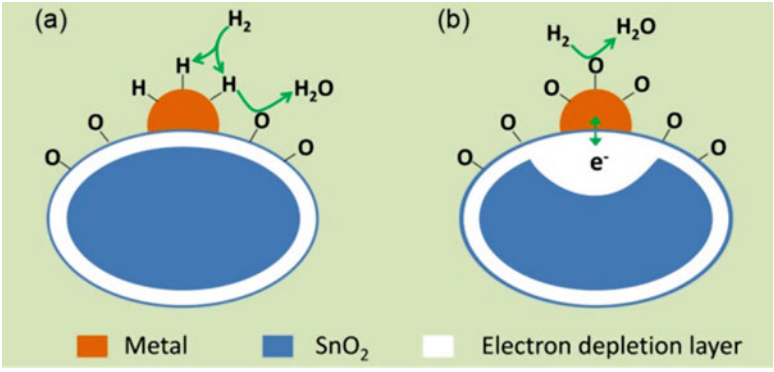

Fig. 7.7 Schematic illustration of (**a**) chemical sensitization and (**b**) electronic sensitization of metal promoters on SnO_2 surface. Reproduced from ref. [93] with permission of Wiley-VCH

spill-over effect, which is well-known in catalytic science. The metal promoter, such as Pt, activates the test gas molecules to facilitate its oxidation on the semiconductor surface. According to Barsan et al., [92] Au also doesn't alter the bulk or surface electronic properties of metal oxide support, hence belonging to the "chemical sensitization" via spill-over effect. In this case the metal promoter does not affect the resistance of the semiconductor and the promoter increases the sensor sensitivity by increasing the reaction rate of the chemical processes. Electronic sensitization (Fig. 7.7b) results from a direct electronic interaction at the interface between the promoter and semiconductor. Specifically, typical promoters (e.g., Ag and Pd) of electronic sensitization are known to form stable oxides (AgO and PdO) in air, and produce an electron-depleted space charge layer on the surface. The electronic sensitization will decrease when the oxide form of metal promoters are reduced to metal by reductive gases.

In another work, Kolmakov et al. [15] have reported that Pd nanoparticles could sensitize the SnO_2 nanowires through spillover effect in addition to electronic

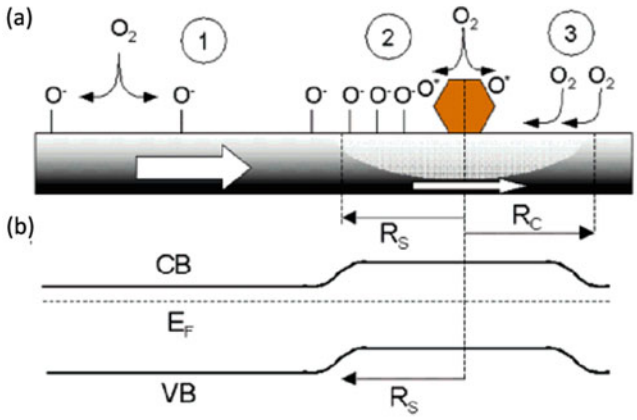

Fig. 7.8 (**a**) Schematic depiction of the three major process taking place at a SnO_2 nanowire/nanobelt surface: (1) ionosorption of oxygen at defect sites of the pristine surface; (2) molecular oxygen dissociation on Pd nanoparticles followed by spillover of the atomic species onto the oxide surface; (3) capture by a Pd nanoparticle of weakly adsorbed molecular oxygen that has diffused along the tin oxide surface to the Pd nanoparticle's vicinity (followed by process 2). R_S is the effective radius of the spillover zone, and R_C is the radius of the collection zone. (**b**) Band diagram of the pristine SnO_2 nanostructure and in the vicinity (and beneath) a Pd nanoparticle. The radius of the depletion region is determined by the radius of the spillover zone. Reproduced from ref. [15] with permission. Copyright 2005, American Chemical Society

sensitization. In contrast to the findings from Barsan et al. [92], they also observed a reduction in conductance of SnO_2 nanowires after loading Au nanoparticles due to formation of baroscopic depletion regions. The decreased conductance is caused by the electron transfer from semiconductor to metal particles induced by nano-Schottky junctions. Figure 7.8 shows both the "chemical sensitization" and "electronic sensitization" of Pd nanoparticles on SnO_2 nanowires. The "electronic mechanism" proposes the formation of depletion zones around the Pd nanoparticles and attributes the improved sensing to the modulation of the nano-Schottky barriers (and hence the width of the conduction channel) due to changes in the oxidation state of the Pd (and therefore its work function) accompanying oxygen adsorption and desorption. Furthermore, the Pd nanoparticles catalytically activate the dissociation of molecular oxygen by spillover effect, "chemical mechanism", whose atomic products then diffuse to the metal oxide support. This process greatly increases both the quantity of oxygen that covering on the SnO_2 surface and the rate at which this dissociation process occurs, resulting in a greater (and faster) degree of electron withdrawal from the SnO_2 (and at a lower temperature) than for the pristine SnO_2 nanowires.

By either chemical sensitization or electronic sensitization, researchers are able to optimize the sensors to selectively detect gas with higher sensitivity and faster response time. In the following parts we will give a detailed overview of the current progress.

7.3.2 *Metal Oxide–Metal Oxide Heteronanowires*

Besides noble metal nanoparticles, various metal oxide nanoparticles also demonstrate great success in improving the sensing features of semiconductors. An appropriate combination of different metal oxide semiconductors to produce heterostructures can lead to enhanced charge transduction and modulated potential barriers at the interface. For heteronanowires constituted by metal oxide nanowires and metal oxide nanoparticles, of central importance is the interface between nanowires and nanoparticles. When two metal oxide semiconductors with different Fermi levels come into contact, the electrons at the higher level will transport across the interface to the lower one until the Fermi energies reach in equilibrium. This leads to a region depleted of charge carriers at the interface. Moreover, a potential energy barrier is generated at the interface due to the band bending which is caused by the difference in original Fermi levels of the materials. Electrons must overcome this barrier in order to cross the interface. Based on the different conductivity type of semiconductors, the coupling of metal oxides can give different heterointerface or heterojunction, e.g. p-n, n-n and p-p. Since n-type metal oxide semiconductors are much more widely used than p-type for gas sensors, [10, 94] within this chapter we mainly focus on the heteronanowires containing n-type metal oxide nanowires as the host.

7.3.2.1 P-N Heteronanowires

P-type metal oxides such as NiO, CuO, Cr_2O_3 and Co_3O_4 are not popularly used for gas sensors due to their low charge carrier mobility and structure instability, [94] however, they can be used as a good promotor in combination with n-type metal oxides to achieve better sensor properties by virtue of p-n heterojunctions. Table 7.2 surveys the gas sensing performances of 1D n-p heterostructures constructed by p-type nanoparticles and n-type nanowires.

The formation of p-n heterojunctions is equivalent to electron–hole recombination in the vicinity of a p–n junctions [103]. Electrons flow from n-type metal oxides to the p-type one and holes flow from p-type metal oxides to the n-type one until the build-up potential prevents such flow. This charge carrier transfer results in a reduction of the hole concentration in the p-type metal oxide and electron concentration in the n-type metal oxide, thus a space charge layer is formed at the heterointerface. Figure 7.9 illustrates the corresponding band structure of heterojunctions in p-Cr_2O_3 nanoparticles/n-SnO_2 nanowires [103]. The width of

Table 7.2 Gas sensing performances of 1D p-n heterostructures

Materials	Test gas	Concentration (ppm)	Sensitivity (S)/Response (R)	Detection limit (ppm)	Temperature (°C)
CuO/WO_3 nanowires [95]	H_2S	100	672.5%	1	300
Co_3O_4/WO_3 nanowires [96]	H_2	2000	6.1	–	200
Co_3O_4/WO_3 nanorods [97]	Acetone	100	5.3	< 6	280
Co_3O_4/ZnO nanorods [17]	NO_2	5	45.4	–	200
NiO/ZnO nanowires [98]	Ethanol	5	29.04	0.05	450
CuO/ZnO nanowires [99]	Ethanol	100	98.8	1	300
CuO/ZnO nanorods [100]	Triethylamine	50	8	< 10	40
CuO/ZnO nanofibers [101]	H_2S	10	18.7	1	230
CuO/SnO_2 nanowires [102]	H_2S	10	15	0.1	300
Cr_2O_3/SnO_2 nanowires [103]	H_2	10	41	–	300
Cr_2O_3/SnO_2 nanowires [19]	Trimethylamine	5	9.87	–	450
NiO/SnO_2 nanowires [104]	H_2S	10	1372	1	300
Cu_2O/SnO_2 nanowires [105]	Benzene	10	12.5	< 5	300
CuO/SnO_2 nanofibers [106]	H_2S	1	23	–	200
CuO/SnO_2 nanofibers [107]	H_2S	10	1.98×10^4	–	300
CuO/In_2O_3 nanowires [108]	H_2S	5	1.16×10^5	1	150

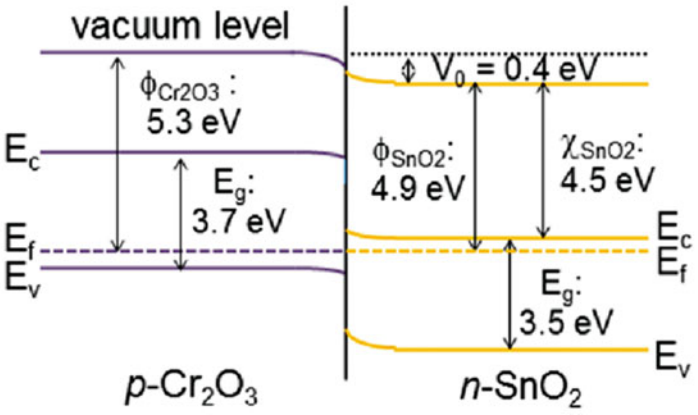

Fig. 7.9 Scheme of the band structure of p-Cr_2O_3/n-SnO_2 heterojunctions. Reproduced from ref. [103] with permission. Copyright 2014, American Chemical Society

the space charge layers (X_n and X_p) induced by the p − n heterojunctions can be calculated using the following equations [46, 103].

$$X_n = \sqrt{\frac{2\varepsilon_n V_0}{q}\left(\frac{N_p}{N_n}\right)\left(\frac{1}{N_n + N_p}\right)}$$

$$X_p = \sqrt{\frac{2\varepsilon_p V_0}{q}\left(\frac{N_n}{N_p}\right)\left(\frac{1}{N_n + N_p}\right)}$$

where ε_n and ε_P, are the static dielectric constant, N_n and N_p carrier concentration of n- and p-type metal oxide semiconductors, respectively, V_0 the contact potential difference between n- and p-type metal oxides.

7.3.2.2 N-N Heteronanowire

Researches have shown that heteronanostructures containing two n-type metal oxides are also quite promising for gas sensing. Table 7.3 lists some typical examples of gas sensors based on n-n heteronanowires.

Unlike the p-n heteronanowires, whose interface at the p–n junction has far few free electrons due to electron-hole recombination, increasing the resistance [45], the interface at an n–n junction simply transfers electrons from the semiconductor with a high Fermi level to the one with a low Fermi level, resulting in a depletion layer in the former and an accumulation layer in the latter. The accumulation layer is further depleted by subsequent oxygen adsorption on the surface, increasing the potential

Table 7.3 Gas sensing performances of 1D n-n heterostructures

Materials	Test gas	Concentration (ppm)	Sensitivity (S)/Response (R)	Detection limit (ppm)	Temperature (°C)
SnO_2/ZnO nanorods [109]	H_2	500	70%	–	400
SnO_2/ZnO nanowires [110]	H_2S	500	1.5	–	250
ZnO/WO_3 nanorods [111]	NO_2	5	281%	–	300
SnO_2/ZnO nanorods [112]	NO_2	500 ppb	13.4	< 200 ppb	Room temp.
ZnO/Fe_2O_3 nanorods [113]	Butanol	100	54.4	–	225
TiO_2/WO_3 nanorods [114]	Acetone	200	7.6	< 10	
ZnO/Fe_2O_3 nanospindles [115]	Ethanol	100	17.8	< 2	280
SnO_2/Fe_2O_3 nanotubes [116]	Ethanol	100	27.45	< 5	200
SnO_2/WO_3 nanowires [117]	H_2	1	137	–	300
Fe_2O_3/In_2O_3 nanowires [118]	Acetone	10	298%	–	200
In_2O_3/SnO_2 nanowires [119]	NO_X	100	8.98	0.1	Room temp.
ZnO/SnO_2 nanotubes [120]	NO_2	5	30.84	0.5	300
In_2O_3/SnO_2 nanofibers [121]	Trimethylamine	10	7.11	< 1	260
La_2O_3/WO_3 nanofibers [122]	Acetone	200	17.8	0.8	350
In_2O_3/WO_3 nanofibers [123]	Acetone	50	12.9	0.4	275
TiO_2/SnO_2 nanofibers [124]	Acetone	100	13.7	< 10	280

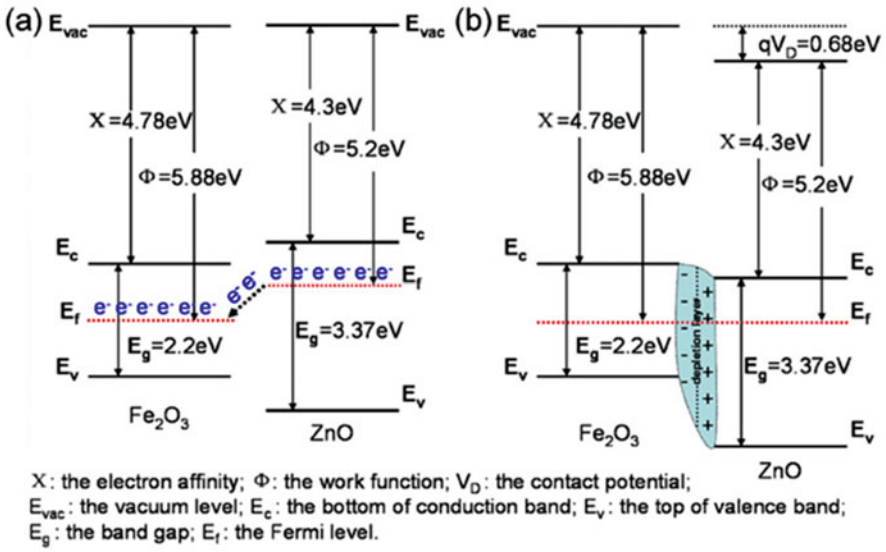

Fig. 7.10 Band structures of (**a**) α-Fe_2O_3 and ZnO and (**b**) α-Fe_2O_3@ZnO heterostructures. Reproduced from ref. [125] with permission of IOP Publishing

energy barrier at the interface. Therefore the sensor response can be enhanced. Fig. 7.10 displays the band structure of a heterostructure based on n-type α-Fe_2O_3 and ZnO [125]. ZnO has a higher Fermi level than α-Fe_2O_3 (Fig. 7.10a), hence the electrons migrate from ZnO to the α-Fe_2O_3 until their Fermi levels equalize, as shown in Fig. 7.10b. The electron transfer leads to the formation of electron depletion layer at the ZnO side. On the surface of ZnO, there is also an electron depletion layer produced by ionized oxygen species. The two conjugated electron depletion layers significantly decrease the carrier concentration in ZnO, making the material highly resistive, and this finally enhances the sensor response.

7.4 Gas Sensing Performances of Heteronanowires

The most important parameters of gas sensor are sensitivity, selectivity, stability and speed (response-recovery rate), namely "4S" and operating temperature. In this section we will overview the advances made in the literature to show how to improve the sensor parameters by using heteronanowires as the sensing layer.

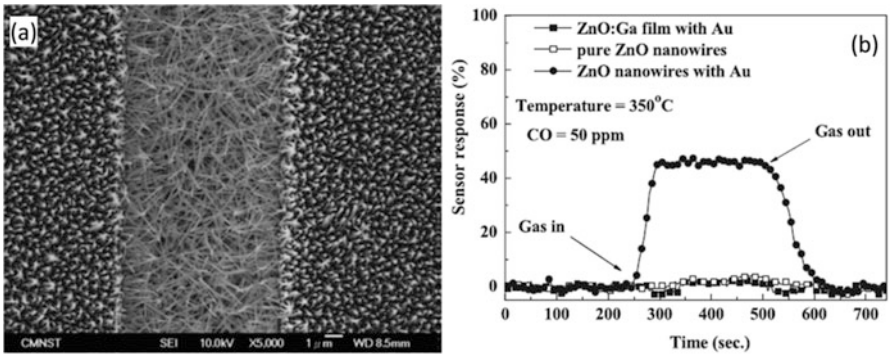

Fig. 7.11 Detector responses of the (**a**) ZnO nanowire-based CO gas sensors; (**b**) responses to 50 ppm CO of different ZnO sensors at 350 °C. Reproduced from ref. [48] with permission of IOP Publishing

7.4.1 Enhanced Sensing Performance of Metal/Metal Oxide Heteronanowires

Numerous works have shown that functionalization of metal oxide nanowires can lead to an enhancement of sensor sensitivity or response. For example, Au-functionalized ZnO nanowires have demonstrated enhanced sensitivity or response to CO, [48] NO_2, [58] H_2S, [52] ethanol, [51, 57] and benzene [53]. In Fig. 7.11, Chang et al. [48] showed that at 350 °C the Au/ZnO nanowires possess a significant higher response to CO than that of pure ZnO nanowire and Au/ZnO film. Other heteronanowires such as Pt/SnO_2 nanowires [64],Pd/ZnO nanorods [60] and Au/In_2O_3 nanowires [75, 77], Pt/TiO_2 nanowires [79] are also reported to enhance the sensor sensitivity or response to CO.

One of the main drawbacks of metal oxide semiconductor sensor materials is the high working temperature, usually between 200 and 400 °C, which is not favorable for obtaining long-term sensor stability. Through metal nanoparticle functionalization, the working temperature of nanowires can be lowered in some cases. For example, Katoch and coworkers [49] reported that the Pt/ZnO nanowires can detect NO_2, CO and benzene at 100 °C with high and fast responses. Lee et al. [75] and Zou et al. [77] show that Au functionalization could result in CO response at room temperature. The FET sensor based on Au/In_2O_3 nanowires [75] is able to detect distinct electrical changes for the CO gas concentration in the range of down to 0.2–5 ppm at room temperature (Fig. 7.12).

For detecting H_2S, Ramgir et al. [54] reported that Au/ZnO nanowires had a much higher response and better selectivity than pure ZnO at room temperature (Fig. 7.13). They also found that the content of Au nanoparticles was crucial to the sensor response. A maximum response is obtained for 1.2 at% Au at room temperature, and this could be attributed to the formation of Au islands ~5 nm size. A remarkable 16-fold increase in the sensor response toward 5 ppm H_2S was obtained by Au

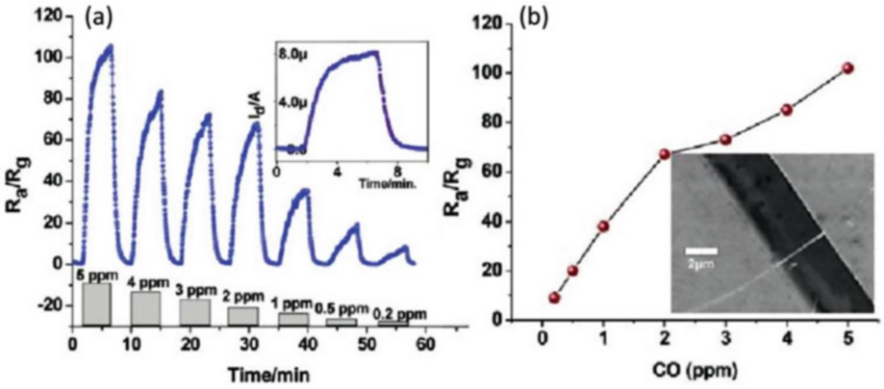

Fig. 7.12 (**a**) Response plot for the Au/In_2O_3 nanowire FET (standard 60 min loading time), when exposed to 5–0.2 ppm CO and inset shows a zoomed view of the I_d-time plot for 5 ppm CO gas, (**b**) sensor response plot for CO gas at room temperature for the same device as shown in the inset. Adapted from ref. [75] with permission. Copyright 2011, American Chemical Society

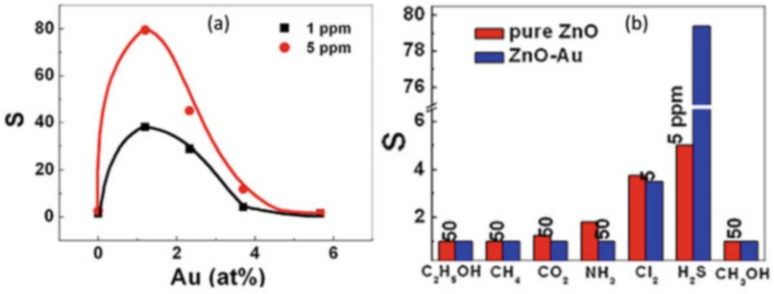

Fig. 7.13 Sensor performance of Au/ZnO nanowires at room temperature, (**a**) sensor response as a function of Au (at%) to H_2S, and (b) selectivity pure and Au (1.2 at%) modified ZnO nanowires samples toward different gases. Reproduced from ref. [54], Copyright 2013, with permission from Elsevier

functionalization. Formation of nano-Schottky type barrier junction at the interface between Au and ZnO has been proposed, and this was correlated with the observance of a higher resistivity and a higher work function (0.2 eV) for Au/ZnO. The enhanced response was thus attributed to the alteration of barrier properties by the adsorption or desorption of adsorbed gas molecules. Decrease in the operating temperature of 1D metal oxide nanostructure-based sensors was also observed in many other material systems such as Pd/SnO_2 nanofibers [72], Pt/In_2O_3 Nanofibers [73], Pt/In_2O_3 nanowires [74], Au/In_2O_3 nanorods [76], and Ag/TiO_2 nanobelts [78], Pd/WO_3 nanowires [126] and Pt/WO_3 nanowires [127].

The selective detection of gas molecules is essential for practical application of gas sensors. Sensors based on semiconductor metal oxides often suffer from a poor discretion among multiple gases. Studies have shown that the sensor selectivity

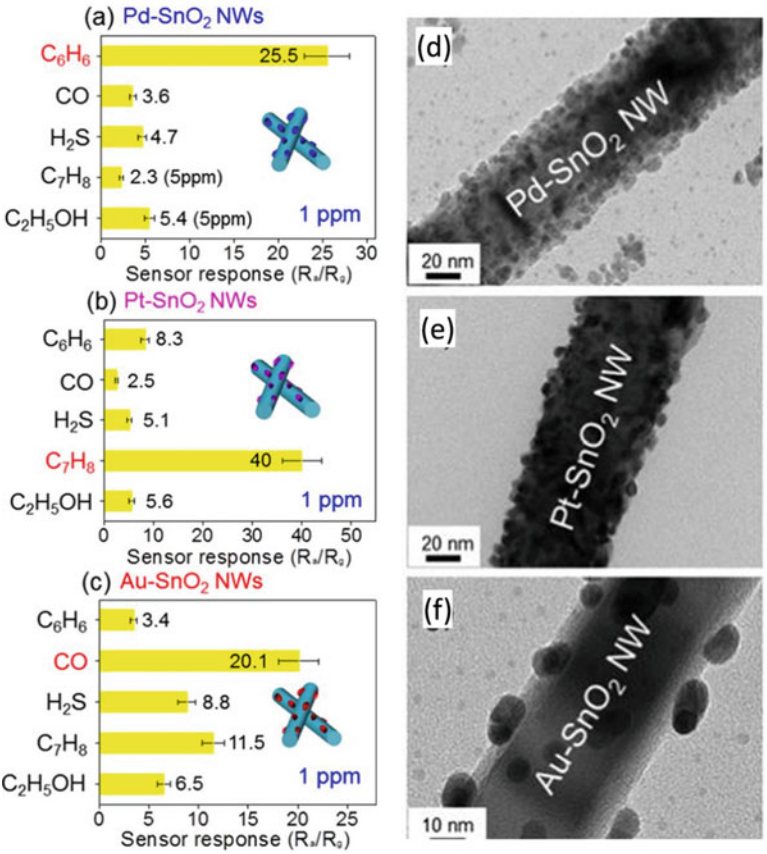

Fig. 7.14 Selective sensing properties of metal-functionalized SnO_2 nanowires: (**a**) Pd, (**b**) Pt, and (**c**) Au; and TEM images: (**d**) Pd/SnO_2, (e) Pt/SnO_2, and (f) Au/SnO_2 nanowires. Reproduced from ref. [64] with permission, Copyright 2016, American Chemical Society

could be optimized by noble metal functionalization towards detecting specific analytes. Kim et al. [64] fabricated a serious of gas sensors based on SnO_2 nanowires functionalized with Pd, Pt and Au nanoparticles using the γ-ray radiolysis technique. Their gas sensing tests (Fig. 7.14) demonstrated that the each noble metal provided exceptional selectivity for a specific gas, i.e., Pd for C_6H_6, Pt for C_7H_8, and Au for CO. They attributed the selective sensing behaviors to the chemical sensitization of noble metals. Briefly, the catalytic oxidation of CO on Au is efficiently improved, the C_6H_6 strongly interacts with Pd, and C_7H_8 tends to bond strongly onto Pt. In another work, Liao and Ho and coworkers [77] designed a gas sensor based on Mg-doped In_2O_3 nanowire FET arrays decorated with Au, Ag, and Pt nanoparticles. This type of gas sensor exhibited a "one key to one lock" selective detection to reducing gases with distinguishable selectivity to CO, C_2H_5OH and H_2, respectively.

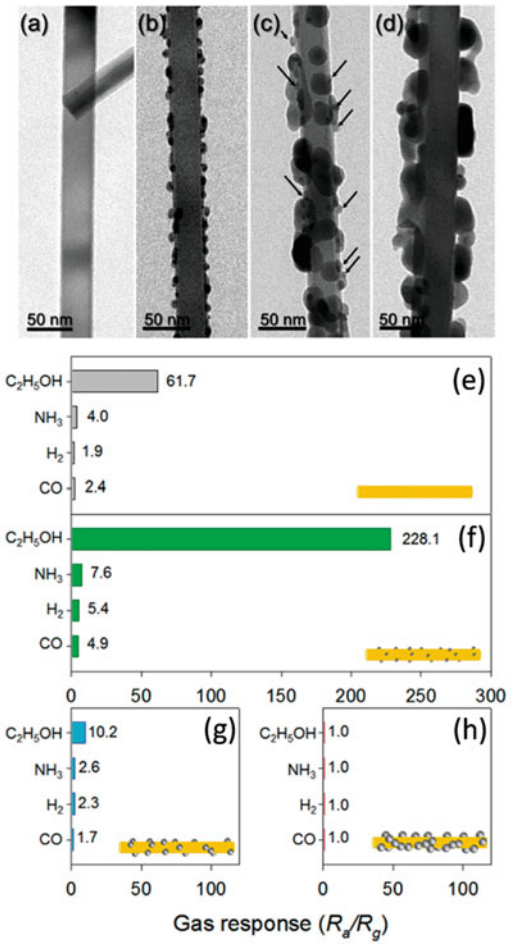

Fig. 7.15 TEM of (**a**) pure SnO_2, (**b**) 5Ag-SnO_2, (**c**) 10Ag-SnO_2, and (**d**) 50Ag-SnO_2 nanowires after heat treatment at 450 °C for 2 h; (e-h) gas responses to 100 ppm various gases at 450 °C. Reproduced from ref. [128] with permission. Copyright 2011, American Chemical Society

For metal nanoparticles functionalization, the loading of metals should be elaborately optimized in order to get the best response. Lee and coworkers [128] studied the effect of the loading of Ag nanoparticles on the detection of ethanol of SnO_2 nanowires. The sensor selectivity to ethanol against NH_3, CO, and H_2 was investigated for three discrete Ag loadings of the SnO_2 nanowires (Fig. 7.15a–d). An optimum Ag loading (Fig. 7.15b, the SnO_2 nanowires were decorated with a high density of 3–8 nm Ag nanoparticles) was observed in terms of both the sensor sensitivity to ethanol and its selectivity for ethanol against the other three gases. In Fig. 7.11f, at the optimum Ag loading, the sensor response to 100 ppm ethanol is 228, significantly higher than that (67) of pure SnO_2 nanowires. It is also seen that higher loading of Ag nanoparticles degraded the sensor response. This might be due to that larger Ag nanoparticles partially or completely connected with each other, as a result, the sensor resistance is not governed by gas sensing properties of SnO_2

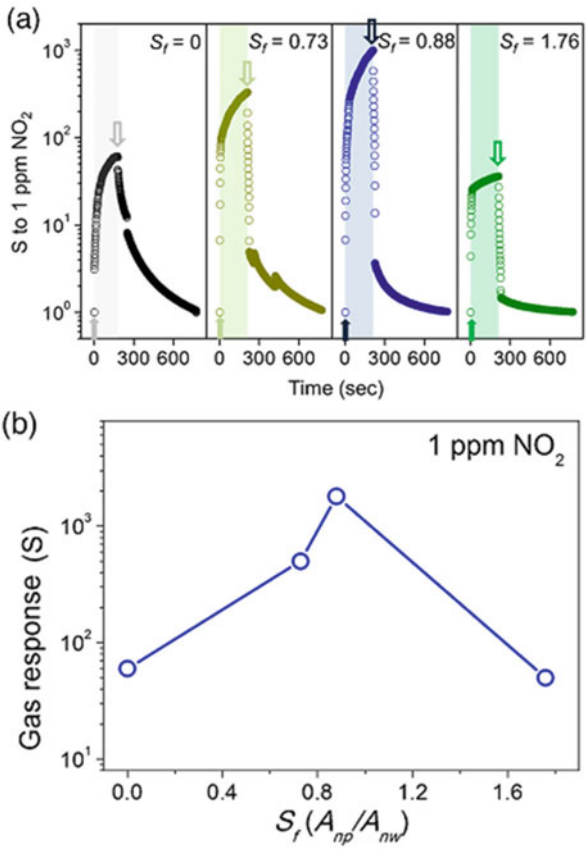

Fig. 7.16 (**a**) Response-recovery curves and (**b**) sensor responses of SnO_2 nanowires functionalized with Ag nanoparticles as a function of S_f. Reproduced from ref. [69], Copyright 2017, with permission from Elsevier

nanowires, but instead it is determined by the insensitive conducting Ag layer. In another work, Kim et al. [69] also studied the NO_2 sensing properties of SnO_2 nanowires as a function of the surface coverage of Ag nanoparticles. The surface coverage (Sf) is defined as the ratio of the average surface area (A_{np}) of Ag NPs to the unit surface area (A_{nw}) of SnO_2 nanowire. As shown in Fig. 7.16, the surface coverage of Ag in the range of 0–1.76 has a large effect on the response to 1 ppm NO_2 of the SnO_2 nanowires. At a S_f of 0.88, the sensor exhibited the highest response, while a further increase of S_f to 1.76 severely deteriorated the response. These works suggest that optimization of S_f or loading of metal is a key parameter in metal nanoparticle–functionalized nanowire sensors.

Response-recovery speed is another important index for gas sensors. The response and recovery times are usually defined as the time for the sensor to reach 90% of the final resistance of the sensor. Metal functionalization of nanowires can also lead to an enhancement of the sensor response-recovery rate. Kim et al. [16] investigated the effect of Pd functionalization on the response-recovery speed of In_2O_3 nanowires for detecting 3 ppm NO_2. In Fig. 7.17, it shows that the response

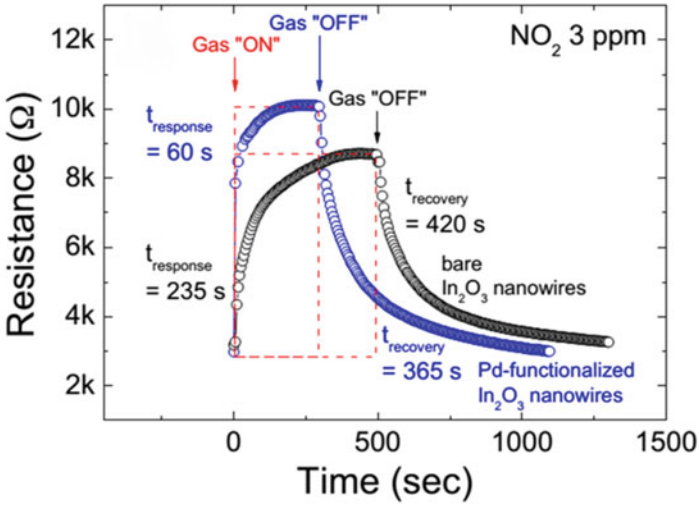

Fig. 7.17 (**a**) Dynamic responses of bare and Pd-functionalized In_2O_3 nanowires for 3 ppm NO_2. Reproduced from ref. [16], Copyright 2011, with permission from Elsevier

time is decreased from 235 S to 60 S due to Pd functionalization, and the recovery time is also greatly shortened.

7.4.2 Enhanced Sensing Performance of P–N Heteronanowires

As shown in Table 7.1, the p-n heteronanowires consist of a variety of material systems, which have demonstrated appealing features in gas sensing. Co_3O_4, NiO, CuO, and Cr_2O_3 are among the most widely used p-type promotors. The unique p-n heterojunction formed at the interface of p-type and n-type semiconductors plays a vital role in gas sensing. By virtue of the p-n heterojunctions, efficient gas sensors for detecting H_2, [96] acetone, [97] trimethylamine, [100] ethanol, [98, 99] CH_4 [110] and NO_2 [17] have been reported. For example, Kim and coworkers [103] examined the Cr_2O_3 nanoparticle-functionalized SnO_2 nanowires for detection of both reducing and oxidizing gases (Fig. 7.18). They found that both pure and functionalized SnO_2 exhibited the highest response to NO_2 at 300 °C in the range of 200–400 °C. The Cr_2O_3/SnO_2 nanowires have a resistance of 5 to 10 times larger than those of the pure SnO_2. This indicates that the electron depletion layer of SnO_2 nanowires is further expanded by the creation of Cr_2O_3/SnO_2 p − n heterojunctions. Notably the Cr_2O_3/SnO_2 nanowires showed greatly improved sensing capabilities to reducing gases (Fig. 7.18c), however, the Cr_2O_3 functionalization was found to deteriorate the oxidizing gas sensing properties of SnO_2 nanowires (Fig. 7.18d).

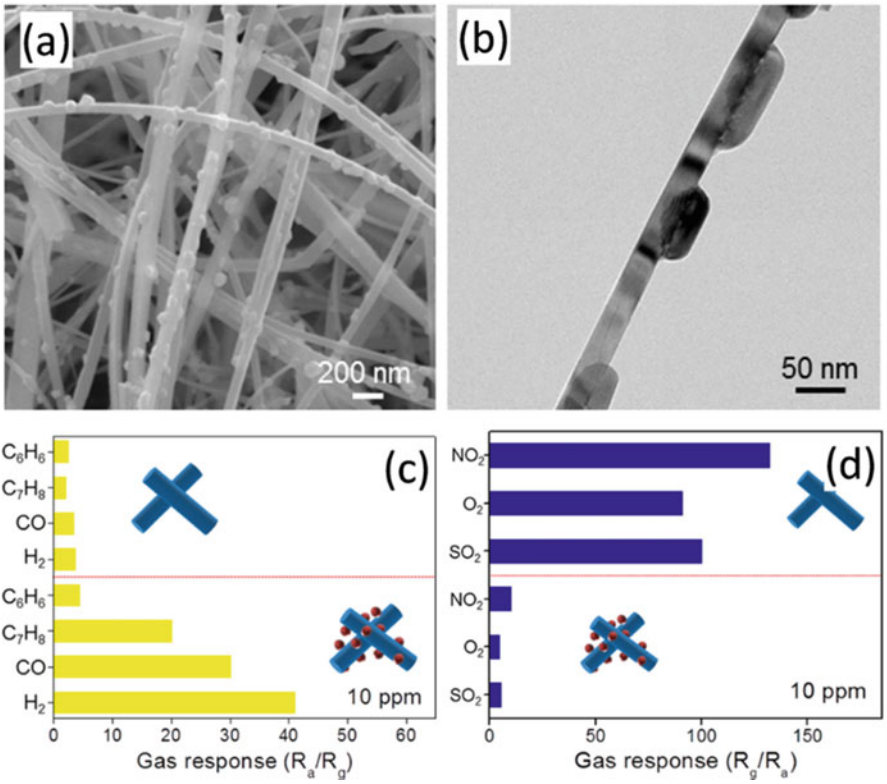

Fig. 7.18 (**a**) SEM and (**b**) TEM images of p-n Cr_2O_3/SnO_2 nanowires, and gas responses to 10 ppm of various gases (**c**) reducing and (**d**) oxidizing gas. Reproduced from ref. [103] with permission. Copyright 2014, American Chemical Society

Hieu and coworkers [104] have applied NiO/SnO_2 nanowires to detect H_2S. The p-n heterojunctions were found to decrease the optimum operating temperature from 350 °C for pure SnO_2 nanowires to 300 °C. Significantly, the NiO/SnO_2 nanowires have a response of 1372 to 10 ppm H_2S, which is 351 higher than that (3.9) of pure SnO_2. Based on the NiO/SnO_2 nanowires, a low concentration of 100 ppb H_2S is also detectable. Such a giant enhancement of H_2S response was attributed to the unique sensing reactions. Upon exposure to H_2S gas at elevated temperatures, the NiO nanoparticles are primarily converted to metallic Ni_3S_2, which is an effective electrical conductor. The formation of metallic Ni_3S_2 can destroy the p-n junction, thus causing a significant decrease in the electrical resistance. A similar mechanism was also widely accepted for CuO-functionalized nanowires for H_2S detection [95, 101, 106, 108], where the formation of metallic CuS greatly altered the sensor resistance during the sensing reactions. Consequently, this mechanism can be used to design H_2S gas sensor materials with a specific selectivity.

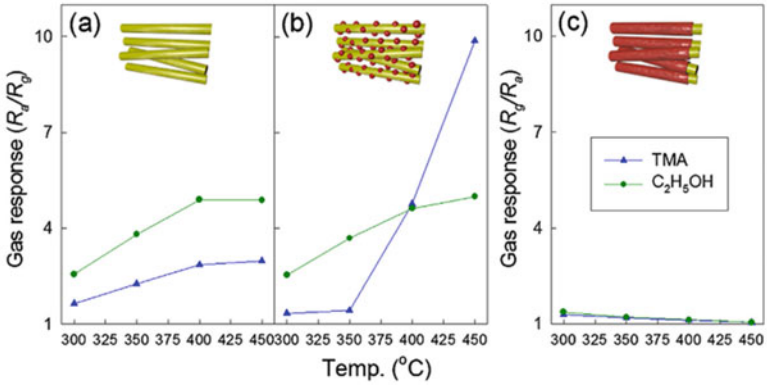

Fig. 7.19 (**a**) Gas responses to 5 ppm C_2H_5OH and 5 ppm trimethylamine at 300–450 °C: (a) pristine SnO_2 nanowires, (**b**) Cr_2O_3-decorated SnO_2 nanowires, and (**c**) core–shell Cr_2O_3/SnO_2 nanowires. Reproduced from ref. [129], Copyright 2014, with permission of Elsevier

Lee and coworkers [129] have shown that Cr_2O_3-decorated SnO_2 nanowires prepared by thermal evaporation were highly sensitive and selective to trimethylamine (Fig. 7.19). The authors found that at temperature of 450 °C the SnO_2 nanowires functionalized with discrete Cr_2O_3 nanoparticles exhibited high response to trimethylamine, when the temperature is below 400 °C, the Cr_2O_3-decorated SnO_2 nanowires are more sensitive to ethanol. They also revealed that if the Cr_2O_3 nanoparticles formed a continuous shell on SnO_2 nanowires, the heteronanowires would lost the discrimination ability to both ethanol and trimethylamine with a negligibly low response. According to the authors, the selective sensing behavior to trimethylamine was attributed, apart from the p-n junction, to the catalytic activity of Cr_2O_3 nanoparticles to promote the selective detection of analyte gas.

7.4.3 Enhanced Sensing Performance of N-N Heteronanowires

In Table 7.3, it shows that the 1D n-n heteronanostructures can be used to detect H_2, NO_2, [112] butanol, [113] acetone, [114] and ethanol [115, 116]. The n-n heterojunctions can lead to enhanced sensor performances based on the chemical or electronic sensitization. For example, Kaneti et al. [113] have demonstrated that ZnO-decorated α-Fe_2O_3 nanorods exhibited excellent sensitivity, selectivity, and stability toward n-butanol gas at a low optimum temperature of 225 °C. Without ZnO functionalization the pure α-Fe_2O_3 nanorods are more sensitive at 250 °C. In particular, the ZnO/α-Fe_2O_3 nanorods has a higher sensitivity compared to pure α-Fe_2O_3 (4 times higher) and ZnO nanorods (2.5 times higher), respectively, as well

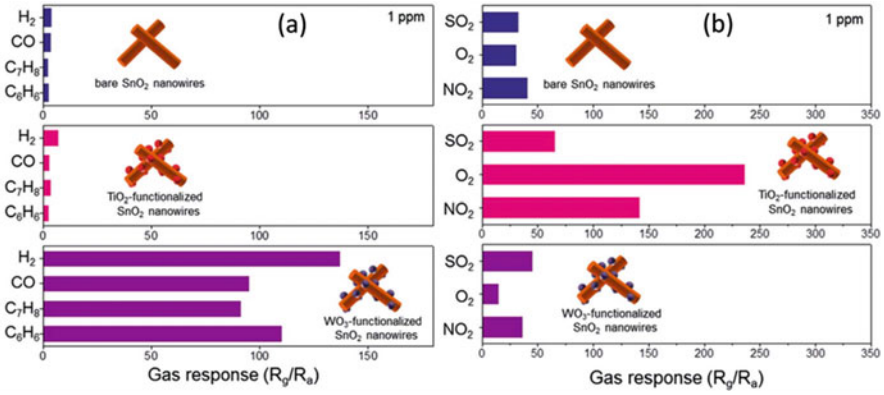

Fig. 7.20 (**a**) gas responses of WO_3/SnO_2 nanowires to 1 ppm various reducing gases and (**b**) gas responses of TiO_2/SnO_2 nanowires to 1 ppm various oxidizing gases (a) 5 ppm trimethylamine at 300 °C. Reproduced from ref. [117] by permission of the Royal Society of Chemistry

as faster response times. In another work from Li et al. [120], it was reported that ZnO nanoparticles improved the response of SnO_2 nanotubes to oxidizing gases, while declined the response to reducing gases. Specifically, the response of ZnO/SnO_2 sensor (1.44) to H_2 was almost nearly one-fifth of the pristine SnO_2 (6.89). While for the oxidizing gas like NO_2, the ZnO/SnO_2 heterojunctions present remarkably enhanced response, being six times higher response (30.84) than that (5.09) of pure SnO_2.

Kuang et al. [110] fabricated a FET gas sensor based on a single SnO_2 nanowire, which was selective to H_2S detection. They showed that at 250 °C the ZnO nanoparticle functionalization could improve the sensor sensitivity to 500 ppm H_2S from 1.26 to 1.50, but in contrast the sensitivity to CO decreased from 1.15 to 1.08, and negligible influence was observed for CH_4.

An acetone sensor with much enhanced response was reported by Lee and coworkers [118]. The good performance was derived from the Fe_2O_3 functionalization of In_2O_3 nanowires. According to the authors the n-n heterojunctions had no effect on the optimum operating temperature, as both pristine and Fe_2O_3 functionalized-In_2O_3 nanowires showed the best response at 200 °C.

Kim et al. [117] recently reported that a selective detection of reducing or oxidizing gases could be realized by functionalizing n-type SnO_2 nanowires with WO_3 or TiO_2 nanoparticles (Fig. 7.20). The key lies in the difference in the work functions of the host nanowires and guest nanoparticles. Specifically, the authors found that the WO_3/SnO_2 nanowires exhibited greatly improved response to reducing gases including H_2, CO, C_7H_8, and C_6H_6. On the other hand, TiO_2 nanoparticles enhanced the oxidizing gas-sensing properties of SnO_2 nanowires. These results are closely associated with the electron flow caused by the work function difference, leading to either compression or expansion of the conduction channel of SnO_2 nanowires along the radial direction. This work intensifies the resistance modulation

of nanowires selectively to either reducing or oxidizing gases, respectively. The approach proposed in this study may contribute significantly to the design of more sensitive nanowire sensors.

7.5 Summary

In this chapter, the utilization of metal oxide nanowires functionalized by metal and metal oxide nanoparticles as the sensing layer for gas sensors has been reviewed. Nanowires with some essential merits such as 1D structure, high crystallinity and tunable diameter are ideal building blocks for gas sensing devices. Due to the large amount of studies published with respect to nanowires and gas sensors, this chapter doesn't attempt to include all the papers to give a complete review. In contrast, a brief overview of gas sensing mechanism and the concept that improve the sensing performances of nanowires, i.e., nanoparticle functionalization, were present. It is concluded that nanoparticle functionalization is an effective method to optimize the sensor performances through either chemical sensitization or electronic sensitization. However challenges are still remaining in this field.

Traditional gas sensing layers are formed by a large quantity of nanoparticles. The nanoparticle units are readily sintered under a long-term working at high temperatures, thus resulting in deteriorated sensor stability. In principle, nanowires offer a better stability compared to the nanoparticle morphology, this should contribute to an improved long-term stability However, it is noted that in most cases, the long-term sensing stability of heteronanowires has not been examined or proved. Thus future efforts are needed to characterize the long-term stability of heteronanowires sensors, especially working in a real operation condition.

Another factor that adds the risk of instability of gas sensors based on heteronanowires is from the nanoparticle promotors. Although the nanoparticle functionalization, as reviewed in this work, could afford significant improvement in sensor sensitivity, the small size of metal nanoparticles makes them unstable. For most metal-functionalized nanowires, a thermal process is usually necessary to stabilize the loading of metal on nanowires. This process is also required to decrease the structural defects in order to enhance the stability of the metal oxides. Thermal treatment or long-term working at a high temperature would lead to a coarsening and aggregation of the metal nanoparticle, thus decreasing the efficiency of chemical sensitization during gas sensing.

The uniform distribution of nanoparticles has a large influence on gas sensing properties of nanowires. The synthetic methods to load nanoparticle are of great importance to guarantee a uniform coverage of nanoparticles with a small size on nanowires. Efforts are still needed to develop more reliable methods.

The understanding of gas sensing mechanism is a central task for sensor scientists. For pristine metal oxides, the basics sensing mechanism has been established and well-understood for decades. However, for a complex system composing of more than two materials, the interactions between each constituents and gas

molecules are also becoming complex. This greatly adds the difficulty for researcher to clarify the gas sensing mechanism. It should be noted that even for the same materials system quite different result can be obtained. As discussed in the context, some works confirm the promotion effect of nanoparticle functionalization in enhancing the sensing performance to reducing gas, but suppressing the sensitivity to oxidizing molecules, while some works obtained an opposite result. Unfortunately, the reasons for such contradictory results are still not clear.

References

1. Kong J, Franklin NR, Zhou C, Chapline MG, Peng S, Cho K, Dai H (2000) Nanotube molecular wires as chemical sensors. Science 287(5453):622–625
2. Favier F, Walter EC, Zach MP, Benter T, Penner RM (2001) Hydrogen sensors and switches from electrodeposited palladium mesowire arrays. Science 293(5538):2227–2231
3. Cui Y, Wei Q, Park H, Lieber CM (2001) Nanowire nanosensors for highly sensitive and selective detection of biological and chemical species. Science 293(5533):1289–1292
4. Law M, Kind H, Messer B, Kim F, Yang PD (2002) Photochemical sensing of NO_2 with SnO_2 nanoribbon nanosensors at room temperature. Angew Chem Int Ed 41(13):2405–2408
5. Kolmakov A, Zhang YX, Cheng GS, Moskovits M (2003) Detection of CO and O_2 using tin oxide nanowire sensors. Adv Mater 15(12):997–1000
6. Shen G, Chen P-C, Ryu K, Zhou C (2009) Devices and chemical sensing applications of metal oxide nanowires. J Mater Chem 19(7):828–839
7. Kolmakov A, Moskovits M (2004) Chemical sensing and catalysis by one-dimensional metal-oxide nanostructures. Annu Rev Mater Res 34:151–180
8. Ramgir NS, Yang Y, Zacharias M (2010) Nanowire-based sensors. Small 6(16):1705–1722
9. Huang X-J, Choi Y-K (2007) Chemical sensors based on nanostructured materials. Sensors Actuators B Chem 122(2):659–671
10. Kim H-J, Lee J-H (2014) Highly sensitive and selective gas sensors using p-type oxide semiconductors: overview. Sensors Actuators B Chem 192:607–627
11. Comini E, Faglia G, Sberveglieri G, Pan ZW, Wang ZL (2002) Stable and highly sensitive gas sensors based on semiconducting oxide nanobelts. Appl Phys Lett 81(10):1869–1871
12. Kolmakov A, Zhang Y, Cheng G, Moskovits M (2003) Detection of CO and O_2 using tin oxide nanowire sensors. Adv Mater 15(12):997–1000
13. Li C, Zhang D, Liu X, Han S, Tang T, Han J, Zhou C (2003) In_2O_3 nanowires as chemical sensors. Appl Phys Lett 82(10):1613–1615
14. Wan Q, Li QH, Chen YJ, Wang TH, He XL, Li JP, Lin CL (2004) Fabrication and ethanol sensing characteristics of ZnO nanowire gas sensors. Appl Phys Lett 84(18):3654–3656
15. Kolmakov A, Klenov DO, Lilach Y, Stemmer S, Moskovits M (2005) Enhanced gas sensing by individual SnO2 nanowires and nanobelts functionalized with Pd catalyst particles. Nano Lett 5(4):667–673
16. Kim SS, Park JY, Choi S-W, Na HG, Yang JC, Kim HW (2011) Enhanced NO_2 sensing characteristics of Pd-functionalized networked In_2O_3 nanowires. J Alloys Compd 509 (37):9171–9177
17. Na CW, Woo H-S, Kim I-D, Lee J-H (2011) Selective detection of NO_2 and C_2H_5OH using a Co_3O_4-decorated ZnO nanowire network sensor. Chem Commun 47(18):5148–5150
18. Katoch A, Choi S-W, Sun G-J, Kim SS (2013) Pt nanoparticle-decorated ZnO nanowire sensors for detecting benzene at room temperature. J Nanosci Nanotechnol 13(10):7097–7099
19. Kwak C-H, Woo H-S, Lee J-H (2014) Selective trimethylamine sensors using Cr_2O_3-decorated SnO_2 nanowires. Sensors Actuators B Chem 204:231–238

20. Park S, Park S, Jung J, Hong T, Lee S, Kim HW, Lee C (2014) H2S gas sensing, properties of CuO-functionalized WO3 nanowires. Ceram Int 40(7):11051–11056
21. Zhang Y, Xiang Q, Xu JQ, Xu PC, Pan QY, Li F (2009) Self-assemblies of Pd nanoparticles on the surfaces of single crystal ZnO nanowires for chemical sensors with enhanced performances. J Mater Chem 19(27):4701–4706
22. Franke ME, Koplin TJ, Simon U (2006) Metal and metal oxide nanoparticles in chemiresistors: does the nanoscale matter? Small 2(1):36–50
23. Hwang I-S, Kim S-J, Choi J-K, Choi J, Ji H, Kim G-T, Cao G, Lee J-H (2010) Synthesis and gas sensing characteristics of highly crystalline ZnO–SnO_2 core–shell nanowires. Sensors Actuators B Chem 148(2):595–600
24. Singh N, Ponzoni A, Gupta RK, Lee PS, Comini E (2011) Synthesis of In_2O_3–ZnO core–shell nanowires and their application in gas sensing. Sensors Actuators B Chem 160(1):1346–1351
25. Park S, An S, Mun Y, Lee C (2013) UV-enhanced NO_2 gas sensing properties of SnO_2-Core/ZnO-Shell nanowires at room temperature. Acs Appl Mater Inter 5(10):4285–4292
26. Kim J-H, Katoch A, Kim SS (2016) Optimum shell thickness and underlying sensing mechanism in p-n CuO-ZnO core-shell nanowires. Sensors Actuators B Chem 222:249–256
27. Wu JM (2010) A room temperature ethanol sensor made from p-type Sb-doped SnO_2 nanowires. Nanotechnology 21(23):235501
28. Ramgir NS, Mulla IS, Vijayamohanan KP (2005) A room temperature nitric oxide sensor actualized from Ru-doped SnO_2 nanowires. Sensors Actuators B Chem 107(2):708–715
29. Wan Q, Wang TH (2005) Single-crystalline Sb-doped SnO_2 nanowires: synthesis and gas sensor application. Chem Commun 30:3841–3843
30. Penner RM (2012) Chemical sensing with nanowires. In: Cooks RG, Yeung ES (eds) Annual review of analytical chemistry, vol 5, pp 461–485. https://doi.org/10.1146/annurev-anchem-062011-143007
31. Chen P-C, Shen G, Zhou C (2008) Chemical sensors and electronic noses based on 1-D metal oxide nanostructures. IEEE T Nanotechnol 7(6):668–682
32. Ponzoni A, Zappa D, Comini E, Sberveglieri V, Faglia G, Sberveglieri G (2012) Metal oxide nanowire gas sensors: application of Conductometric and surface ionization architectures. In: Del Rosso R, Pierucci S, Klemes JJ (eds) Nose 2012: 3rd international conference on environmental odour monitoring and control. Chemical engineering transactions 30:31–36. doi:https://doi.org/10.3303/cet1230006
33. Ramgir N, Datta N, Kaur M, Kailasaganapathi S, Debnath AK, Aswal DK, Gupta SK (2013) Metal oxide nanowires for chemiresistive gas sensors: issues, challenges and prospects. Colloid Surface A 439:101–116
34. Sawicka KM, Prasad AK, Gouma PI (2005) Metal oxide nanowires for use in chemical sensing applications. Sens Lett 3(1):31–35
35. Fang X, Hu L, Ye C, Zhang L (2010) One-dimensional inorganic semiconductor nanostructures: a new carrier for nanosensors. Pure Appl Chem 82(11):2185–2198
36. Comini E, Baratto C, Concina I, Faglia G, Falasconi M, Ferroni M, Galstyan V, Gobbi E, Ponzoni A, Vomiero A, Zappa D, Sberveglieri V, Sberveglieri G (2013) Metal oxide nanoscience and nanotechnology for chemical sensors. Sensors Actuators B Chem 179:3–20
37. Zhai T, Yao J (2012) One-dimensional nanostructures: principles and applications. Wiley, Hoboken
38. Chen X, Wong CK, Yuan CA, Zhang G (2013) Nanowire-based gas sensors. Sensors Actuators B Chem 177:178–195
39. Sysoev VV, Schneider T, Goschnick J, Kiselev I, Habicht W, Hahn H, Strelcov E, Kolmakov A (2009) Percolating SnO_2 nanowire network as a stable gas sensor: direct comparison of long-term performance versus SnO_2 nanoparticle films. Sensors Actuators B Chem 139 (2):699–703
40. Zhang D, Liu Z, Li C, Tang T, Liu X, Han S, Lei B, Zhou C (2004) Detection of NO_2 down to ppb levels using individual and multiple In_2O_3 nanowire devices. Nano Lett 4(10):1919–1924

41. Shimizu Y, Egashira M (1999) Basic aspects and challenges of semiconductor gas sensors. MRS Bull 24(6):18–24
42. Barsan N, Weimar U (2001) Conduction model of metal oxide gas sensors. J Electroceram 7 (3):143–167
43. Yamazoe N (1991) New approaches for improving semiconductor gas sensors. Sensors Actuators B Chem 5:7–19
44. Yamazoe N, Sakai G, Shimanoe K (2003) Oxide semiconductor gas sensors. Catal Surv Jpn 7 (1):63–75
45. Miller DR, Akbar SA, Morris PA (2014) Nanoscale metal oxide-based heterojunctions for gas sensing: a review. Sensors Actuators B Chem 204:250–272
46. Li T, Zeng W, Wang Z (2015) Quasi-one-dimensional metal-oxide-based heterostructural gas-sensing materials: a review. Sensors Actuators B Chem 221:1570–1585
47. Hsueh T-J, Chang S-J, Hsu C-L, Lin Y-R, Chen IC (2007) Highly sensitive ZnO nanowire ethanol sensor with Pd adsorption. Appl Phys Lett 91(5):053111
48. Chang S-J, Hsueh T-J, Chen IC, Huang B-R (2008) Highly sensitive ZnO nanowire CO sensors with the adsorption of Au nanoparticles. Nanotechnology 19(17):175502
49. Katoch A, Choi S-W, Sun G-J, Kim SS (2015) Low temperature sensing properties of Pt nanoparticle-functionalized networked ZnO nanowires. J Nanosci Nanotechnol 15 (1):330–333
50. Liang Y-C, Liao W-K, Deng X-S (2014) Synthesis and substantially enhanced gas sensing sensitivity of homogeneously nanoscale Pd- and Au-particle decorated ZnO nanostructures. J Alloys Compd 599:87–92
51. Guo J, Zhang J, Zhu M, Ju D, Xu H, Cao B (2014) High-performance gas sensor based on ZnO nanowires functionalized by Au nanoparticles. Sensors Actuators B Chem 199:339–345
52. Hosseini ZS, Mortezaali A, Zad AI, Fardindoost S (2015) Sensitive and selective room temperature H2S gas sensor based on Au sensitized vertical ZnO nanorods with flower-like structures. J Alloys Compd 628:222–229
53. Wang L, Wang S, Xu M, Hu X, Zhang H, Wang Y, Huang W (2013) A Au-functionalized ZnO nanowire gas sensor for detection of benzene and toluene. Phys Chem Chem Phys 15 (40):17179–17186
54. Ramgir NS, Sharma PK, Datta N, Kaur M, Debnath A, Aswal D, Gupta S (2013) Room temperature H_2S sensor based on Au modified ZnO nanowires. Sensors Actuators B Chem 186:718–726
55. Liu X, Zhang J, Guo X, Wu S, Wang S (2010) Amino acid-assisted one-pot assembly of Au, Pt nanoparticles onto one-dimensional ZnO microrods. Nanoscale 2(7):1178–1184
56. Ramgir NS, Kaur M, Sharma PK, Datta N, Kailasaganapathi S, Bhattacharya S, Debnath AK, Aswal DK, Gupta K (2013) Ethanol sensing properties of pure and Au modified ZnO nanowires. Sensors Actuators B Chem 187:313–318
57. Suo C, Gao C, Wu X, Zuo Y, Wang X, Jia J (2015) Ag-decorated ZnO nanorods prepared by photochemical deposition and their high selectivity to ethanol using conducting oxide electrodes. RSC Adv 5(112):92107–92113
58. Ponnuvelu DV, Pullithadathil B, Prasad AK, Dhara S, Ashok A, Mohamed K, Tyagi AK, Raja B (2015) Rapid synthesis and characterization of hybrid ZnO@Au core-shell nanorods for high performance, low temperature NO_2 gas sensor applications. Appl Surf Sci 355:726–735
59. Zhang YA, Xu JQ, Xu PC, Zhu YH, Chen XD, Yu WJ (2010) Decoration of ZnO nanowires with Pt nanoparticles and their improved gas sensing and photocatalytic performance. Nanotechnology 21(28):7
60. Rai P, Yu YT (2013) Citrate-assisted one-pot assembly of palladium nanoparticles onto ZnO nanorods for CO sensing application. Mater Chem Phys 142(2–3):545–548
61. Rai P, Kim YS, Song HM, Song MK, Yu YT (2012) The role of gold catalyst on the sensing behavior of ZnO nanorods for CO and NO_2 gases. Sensors Actuators B Chem 165(1):133–142

62. Shen Y, Yamazaki T, Liu Z, Meng D, Kikuta T, Nakatani N, Saito M, Mori M (2009) Microstructure and H_2 gas sensing properties of undoped and Pd-doped SnO_2 nanowires. Sensors Actuators B Chem 135(2):524–529
63. Fu DY, Zhu CL, Zhang XT, Li CY, Chen YJ (2016) Two-dimensional net-like SnO_2/ZnO heteronanostructures for high-performance H_2S gas sensor. J Mater Chem A 4(4):1390–1398
64. Kim J-H, Wu P, Kim HW, Kim SS (2016) Highly selective sensing of CO, C_6H_6, and C_7H_8 gases by catalytic functionalization with metal nanoparticles. Acs Appl Mater Int 8 (11):7173–7183
65. Do Dang T, Nguyen Duc H, Pham Van T, Nguyen Van D, Dao TD, Chung HV, Nagao T, Nguyen Van H (2014) Effective decoration of Pd nanoparticles on the surface of SnO_2 nanowires for enhancement of CO gas-sensing performance. J Hazard Mater 265:124–132
66. Park S, Kim S, Ko H, Lee C (2014) Dependence of the selectivity of SnO_2 nanorod gas sensors on functionalization materials. Appl Phys a-Mater 117(3):1259–1267
67. Lin Y, Wei W, Li YJ, Li F, Zhou JR, Sun DM, Chen Y, Ruan SP (2015) Preparation of Pd nanoparticle-decorated hollow SnO_2 nanofibers and their enhanced formaldehyde sensing properties. J Alloys Compd 651:690–698
68. Kou X, Xie N, Chen F, Wang T, Guo L, Wang C, Wang Q, Ma J, Sun Y, Zhang H, Lu G (2017) Superior acetone gas sensor based on electrospun SnO2 nanofibers by Rh doping. Sens Actuators B 256:861–869
69. Abideen ZU, Kim J-H, Kim SS (2017) Optimization of metal nanoparticle amount on SnO_2 nanowires to achieve superior gas sensing properties. Sensors Actuators B Chem 238:374–380
70. Huang H, Ong C, Guo J, White T, Tse MS, Tan OK (2010) Pt surface modification of SnO_2 nanorod arrays for CO and H_2 sensors. Nanoscale 2(7):1203–1207
71. Choi S-W, Jung S-H, Kim SS (2011) Significant enhancement of the NO_2 sensing capability in networked SnO_2 nanowires by au nanoparticles synthesized via gamma-ray radiolysis. J Hazard Mater 193:243–248
72. Wang ZJ, Li ZY, Jiang TT, Xu XR, Wang C (2013) Ultrasensitive hydrogen sensor based on Pd-0-loaded SnO_2 electrospun nanofibers at room temperature. Acs Appl Mater Int 5 (6):2013–2021
73. Zheng W, Lu XF, Wang W, Li ZY, Zhang HN, Wang ZJ, Xu XR, Li SY, Wang C (2009) Assembly of Pt nanoparticles on electrospun In_2O_3 nanofibers for H2S detection. J Colloid Interface Sci 338(2):366–370
74. Kim SS, Park JY, Choi SW, Kim HS, Na HG, Yang JC, Kim HW (2010) Significant enhancement of the sensing characteristics of In_2O_3 nanowires by functionalization with Pt nanoparticles. Nanotechnology 21(41):7
75. Singh N, Gupta RK, Lee PS (2011) Gold-nanoparticle-functionalized In2O3 nanowires as CO gas sensors with a significant enhancement in response. Acs Appl Mater Int 3(7):2246–2252
76. Xing R, Xu L, Song J, Zhou C, Li Q, Liu D, Song HW (2015) Preparation and gas sensing properties of In2O3/Au Nanorods for detection of volatile organic compounds in exhaled breath. Sci Rep 5 5:10717
77. Zou XM, Wang JL, Liu XQ, Wang CL, Jiang Y, Wang Y, Xiao XH, Ho JC, Li JC, Jiang CZ, Fang Y, Liu W, Liao L (2013) Rational Design of sub-Parts per million specific gas sensors Array based on metal nanoparticles decorated nanowire enhancement-mode transistors. Nano Lett 13(7):3287–3292
78. Hu PQ, Du GJ, Zhou WJ, Cui JJ, Lin JJ, Liu H, Liu D, Wang JY, Chen SW (2010) Enhancement of ethanol vapor sensing of TiO_2 Nanobelts by surface engineering. Acs Appl Mater Int 2(11):3263–3269
79. Jin C, Kim H, Choi S-W, Kim SS, Lee C (2014) Synthesis, structure, and gas-sensing properties of Pt-functionalized TiO2 nanowire sensors. J Nanosci Nanotechnol 14 (8):5833–5838
80. Meng D, Yamazaki T, Kikuta T (2014) Preparation and gas sensing properties of undoped and Pd-doped TiO2 nanowires. Sensors Actuators B Chem 190:838–843

81. Sennik E, Soysal U, Ozturk ZZ (2014) Pd loaded spider-web TiO_2 nanowires: fabrication, characterization and gas sensing properties. Sensors Actuators B Chem 199:424–432
82. Sennik E, Alev Ol; Zturk ZZ (2016) The effect of Pd on the H_2 and VOC sensing properties of TiO_2 nanorods. Sensors Actuators B Chem 229:692–700
83. Xiang Q, Meng GF, Zhao HB, Zhang Y, Li H, Ma WJ, Xu JQ (2010) Au nanoparticle modified WO_3 Nanorods with their enhanced properties for Photocatalysis and gas sensing. J Phys Chem C 114(5):2049–2055
84. Liu X, Zhang J, Yang T, Guo X, Wu S, Wang S (2011) Synthesis of Pt nanoparticles functionalized WO_3 nanorods and their gas sensing properties. Sensors Actuators B Chem 156(2):918–923
85. Tong PV, Hoa ND, Duy NV, Dang Thi Thanh L, Hieu NV (2016) Enhancement of gas-sensing characteristics of hydrothermally synthesized WO_3 nanorods by surface decoration with Pd nanoparticles. Sensors Actuators B Chem 223:453–460
86. Choi S-J, Chattopadhyay S, Kim JJ, Kim S-J, Tuller HL, Rutledge GC, Kim I-D (2016) Coaxial electrospinning of WO_3 nanotubes functionalized with bio-inspired Pd catalysts and their superior hydrogen sensing performance. Nanoscale 8(17):9159–9166
87. Nguyen Minh V, Kim D, Kim H (2015) Porous Au-embedded WO_3 nanowire structure for efficient detection of CH_4 and H_2S. Sci Rep 5 5:11040
88. Kruefu V, Wisitsoraat A, Tuantranont A, Phanichphant S (2015) Ultra-sensitive H_2S sensors based on hydrothermal/impregnation-made Ru-functionalized WO_3 nanorods. Sensors Actuators B Chem 215:630–636
89. Chavez F, Perez-Sanchez GF, Goiz O, Zaca-Moran P, Pena-Sierra R, Morales-Acevedo A, Felipe C, Soledad-Priego M (2013) Sensing performance of palladium-functionalized WO_3 nanowires by a drop-casting method. Appl Surf Sci 275:28–35
90. Gunawan P, Mei L, Teo J, Ma JM, Highfield J, Li QH, Zhong ZY (2012) Ultrahigh sensitivity of Au/1D alpha-Fe_2O_3 to acetone and the sensing mechanism. Langmuir 28(39):14090–14099
91. Wang SR, Zhang HX, Wang YS, Wang LW, Gong Z (2014) Facile one-pot synthesis of Au nanoparticles decorated porous alpha-Fe_2O_3 nanorods for in situ detection of VOCs. RSC Adv 4(1):369–373
92. Hubner M, Koziej D, Grunwaldt J-D, Weimar U, Barsan N (2012) An Au clusters related spill-over sensitization mechanism in SnO_2-based gas sensors identified by operando HERFD-XAS, work function changes, DC resistance and catalytic conversion studies. Phys Chem Chem Phys 14(38):13249–13254
93. Zhang J, Liu X, Neri G, Pinna N (2016) Nanostructured materials for room-temperature gas sensors. Adv Mater 28(5):795–831
94. Korotcenkov G (2007) Metal oxides for solid-state gas sensors: what determines our choice? Mater Sci Eng B 139(1):1–23
95. Park S, Park S, Jung J, Hong T, Lee S, Kim HW, Lee C (2014) H_2S gas sensing properties of CuO-functionalized WO_3 nanowires. Ceram Int 40(7):11051–11056
96. Park S, Sun G-J, Kheel H, Hyun SK, Jin C, Lee C (2016) Hydrogen gas sensing of Co_3O_4-decorated WO_3 nanowires. Met Mater Int 22(1):156–162
97. Zhao XD, Ji HM, Jia QQ, Wang MJ (2015) A nanoscale Co_3O_4-WO_3 p-n junction sensor with enhanced acetone responsivity. J Mater Sci-Mater Electron 26(10):8217–8223
98. Na CW, Woo H-S, Lee J-H (2012) Design of highly sensitive volatile organic compound sensors by controlling NiO loading on ZnO nanowire networks. RSC Adv 2(2):414–417
99. Zhang Y-B, Yin J, Li L, Zhang L-X, Bie L-J (2014) Enhanced ethanol gas-sensing properties of flower-like p-CuO/n-ZnO heterojunction nanorods. Sensors Actuators B Chem 202:500–507
100. Xu Q, Ju D, Zhang Z, Yuan S, Zhang J, Xu H, Cao B (2016) Near room-temperature triethylamine sensor constructed with CuO/ZnO P-N heterostructural nanorods directly on flat electrode. Sensors Actuators B Chem 225:16–23
101. Zhao M, Wang X, Ning L, Jia J, Li X, Cao L (2011) Electrospun cu-doped ZnO nanofibers for H_2S sensing. Sensors Actuators B Chem 156(2):588–592

102. Sun GJ, Choi SW, Katoch A, Wu P, Kim SS (2013) Bi-functional mechanism of H_2S detection using CuO-SnO_2 nanowires. J Mater Chem C 1(35):5454–5462
103. Choi S-W, Katoch A, Kim J-H, Kim SS (2014) Prominent reducing gas-sensing performances of n-SnO_2 nanowires by local creation of p-n heterojunctions by functionalization with p-Cr_2O_3 nanoparticles. Acs Appl Mater Inter 6(20):17723–17729
104. Hieu NV, Phung THV, Nhan LT, Duy NV, Hoa ND (2012) Giant enhancement of H_2S gas response by decorating n-type SnO_2 nanowires with p-type NiO nanoparticles. Appl Phys Lett 101(25):253106
105. Kim J-H, Katoch A, Kim S-H, Kim SS (2015) Chemiresistive sensing behavior of SnO_2 (n)–Cu_2O (p) Core–Shell nanowires. Acs Appl Mater Int 7(28):15351–15358
106. Zhao Y, He X, Li J, Gao X, Jia J (2012) Porous CuO/SnO_2 composite nanofibers fabricated by electrospinning and their H_2S sensing properties. Sensors Actuators B Chem 165(1):82–87
107. Choi S-W, Zhang J, Akash K, Kim SS (2012) H2S sensing performance of electrospun CuO-loaded SnO2 nanofibers. Sensors Actuators B Chem 169:54–60
108. Liang X, Kim T-H, Yoon J-W, Kwak C-H, Lee J-H (2015) Ultrasensitive and ultraselective detection of H_2S using electrospun CuO-loaded In_2O_3 nanofiber sensors assisted by pulse heating. Sensors Actuators B Chem 209:934–942
109. Tien LC, Norton DP, Gila BP, Pearton SJ, Wang HT, Kang BS, Ren F (2007) Detection of hydrogen with SnO_2-coated ZnO nanorods. Appl Surf Sci 253(10):4748–4752
110. Kuang Q, Lao C-S, Li Z, Liu Y-Z, Xie Z-X, Zheng L-S, Wang ZL (2008) Enhancing the photon- and gas-sensing properties of a single SnO_2 nanowire based nanodevice by nanoparticle surface functionalization. J Phys Chem C 112(30):11539–11544
111. An S, Park S, Ko H, Lee C (2012) Enhanced NO_2 gas sensing properties of WO_3 nanorods encapsulated with ZnO. Appl Phys a-Mater 108(1):53–58
112. Lu GY, Xu J, Sun JB, Yu YS, Zhang YQ, Liu FM (2012) UV-enhanced room temperature NO_2 sensor using ZnO nanorods modified with SnO_2 nanoparticles. Sensors Actuators B Chem 162(1):82–88
113. Kaneti YV, Zakaria QMD, Zhang ZJ, Chen CY, Yue J, Liu MS, Jiang XC, Yu AB (2014) Solvothermal synthesis of ZnO-decorated alpha-Fe_2O_3 nanorods with highly enhanced gas-sensing performance toward n-butanol. J Mater Chem A 2(33):13283–13292
114. Zhang HX, Wang SR, Wang YS, Yang JD, Gao XL, Wang LW (2014) TiO_2(B) nanoparticle-functionalized WO_3 nanorods with enhanced gas sensing properties. Phys Chem Chem Phys 16(22):10830–10836
115. Zhang JX, Zhu GX, Shen XP, Ji ZY, Chen KM (2014) Alpha-Fe_2O_3 nanospindles loaded with ZnO nanocrystals: synthesis and improved gas sensing performance. Cryst Res Technol 49 (7):452–459
116. Zhao CH, Hu WQ, Zhang ZX, Zhou JY, Pan XJ, Xie EQ (2014) Effects of SnO_2 additives on nanostructure and gas-sensing properties of alpha-Fe_2O_3 nanotubes. Sensors Actuators B Chem 195:486–493
117. Choi SW, Katoch A, Kim JH, Kim SS (2015) Striking sensing improvement of n-type oxide nanowires by electronic sensitization based on work function difference. J Mater Chem C 3 (7):1521–1527
118. Kim S, Park S, Sun GJ, Hyun SK, Kim KK, Lee C (2015) Enhanced acetone gas sensing performance of the multiple-networked Fe_2O_3-functionalized In_2O_3 nanowire sensor. Curr Appl Phys 15(8):947–952
119. Xu S, Gao J, Wang LL, Kan K, Xie Y, Shen PK, Li L, Shi KY (2015) Role of the heterojunctions in In_2O_3-composite SnO_2 nanorod sensors and their remarkable gas-sensing performance for NO_x at room temperature. Nanoscale 7(35):14643–14651
120. Diao KD, Huang YP, Zhou MJ, Zhang JC, Tang YJ, Wang SX, Liu TX, Cui XD (2016) Selectively enhanced sensing performance for oxidizing gases based on ZnO nanoparticle-loaded electrospun SnO2 nanotube heterostructures. RSC Adv 6(34):28419–28427

121. Li F, Gao X, Wang R, Zhang T, Lu G, Barsan N (2016) Design of Core–Shell Heterostructure Nanofibers with different work function and their sensing properties to trimethylamine. Acs Appl Mater Int 8(30):19799–19806
122. Feng C, Wang C, Cheng P, Li X, Wang B, Guan Y, Ma J, Zhang H, Sun Y, Sun P, Zheng J, Lu G (2015) Facile synthesis and gas sensing properties of La2O3–WO3 nanofibers. Sens Actuators B 221(C):434–442
123. Feng C, Li X, Ma J, Sun Y, Wang C, Sun P, Zheng J, Lu G (2015) Facile synthesis and gas sensing properties of In_2O_3–WO_3 heterojunction nanofibers. Sensors Actuators B Chem 209:622–629
124. Li F, Gao X, Wang R, Zhang T, Lu G (2017) Study on TiO2-SnO2 core-shell heterostructure nanofibers with different work function and its application in gas sensor. Sens Actuators B 248 (C):812–819
125. Zhang J, Liu X, Wang L, Yang T, Guo X, Wu S, Wang S, Zhang S (2011) Synthesis and gas sensing properties of alpha-Fe_2O_3@ZnO core-shell nanospindles. Nanotechnology 22 (18):185501
126. Kukkola J, Mohl M, Leino A-R, Maklin J, Halonen N, Shchukarev A, Konya Z, Jantunen H, Kordas K (2013) Room temperature hydrogen sensors based on metal decorated WO_3 nanowires. Sensors Actuators B Chem 186:90–95
127. Zhu LF, She JC, Luo JY, Deng SZ, Chen J, Xu NS (2010) Study of physical and chemical processes of H_2 sensing of Pt-coated WO_3 nanowire films. J Phys Chem C 114 (36):15504–15509
128. Hwang I-S, Choi J-K, Woo H-S, Kim S-J, Jung S-Y, Seong T-Y, Kim I-D, Lee J-H (2011) Facile control of C_2H_5OH sensing characteristics by decorating discrete ag nanoclusters on SnO_2 nanowire networks. Acs Appl Mater Int 3(8):3140–3145
129. Kwak C-H, Woo H-S, Lee J-H (2014) Selective trimethylamine sensors using Cr2O3-decorated SnO2 nanowires. Sens Actuators B 204(Supplement C):231–238